Numerical simulation of nonlinear wave interactions with linearly sheared currents

Citation for published version:
Chen, H & Zou, Q 2015, Numerical simulation of nonlinear wave interactions with linearly sheared currents. in *Proceedings of the 25th International Ocean and Polar Engineering Conference.* International Society of Offshore and Polar Engineers, pp. 538-542, 25th International Ocean and Polar Engineering Conference 2015, Kona, Big Island, United States, 21/06/15.

Published In:
Proceedings of the 25th International Ocean and Polar Engineering Conference

Proceedings of the Twenty-fifth (2015) International Ocean and Polar Engineering Conference
Kona, Big Island, Hawaii, USA, June 21-26, 2015 **www.isope.org**

ISBN 978-1-880653-89-0; ISSN 1098-6189

Numerical Simulation of Nonlinear Wave Interactions with Linearly Sheared Currents

Haifei Chen and Qingping Zou
Department of Civil and Environmental Engineering, University of Maine
Orono, Maine, USA

ABSTRACT

A numerical investigation of nonlinear wave interactions with approximately linearly sheared currents is presented. The numerical model is based on the Navier-Stokes Solver, and the Volume of Fluid method is applied to capture the water wave surface. The numerical model is validated with the experimental measurements in the case of a uniform current and a linearly sheared current. The effects of wave nonlinearity and current shear on the water surface profiles are examined. It was found that in the presence of the current shear, the wave crests are sharper and troughs flatter for the following current; while for the opposing current, the troughs tend to be deeper. The effect is more pronounced when the wave steepness increases.

KEY WORDS: Wave-current interaction; CFD; linearly sheared currents; nonlinear waves; current shear.

INTRODUCTION

Waves and currents coexist in most marine environments. The interactions between these flows have been studied for decades, both theoretically and experimentally. The review articles by Peregrine and Jonsson (1983), Jonsson (1990) and Thomas and Klopman (1997) document well the previous studies on this topic.

Waves traveling over currents experience a modulation in their kinematics. In the simplest case involving a current which is uniform with depth, the Doppler shift (Fenton, 1985) is a common concept to explain such modulations in wave dispersion and the associated water particle kinematics. When the current profile is not uniform and has some weak or strong shear across the water depth, the resulting wave motions become more complex. Several studies (Thomas 1981, 1990; Swan, 1990; Swan, Cummins and James, 2001) have established the importance of the current shear, or vorticity, in affecting the wave kinematics and water surface elevations.

In the past few decades, some weakly nonlinear analytical solutions (Tsao, 1959; Kishida and Sobey, 1988) have been obtained for a linearly sheared current, and it's shown that the current shear produces changes in the water surface elevation. Nonlinear inviscid numerical models, e.g. Dalrymple (1974) and Thomas (1990), have also been proposed for weakly and strongly sheared current. The approach by Dalrymple (1974) divides the water column into a number of discrete layers, approximating the current in each layer by a linear shear, and uses a Fourier series expansion of the stream function to represent the resulting wave form.

Most of the early experimental studies (Brevik, 1980; Kemp and Simons 1982, 1983; Umeyama 2005, 2009) have considered waves on a uniform current. In perhaps the most detailed investigation of current shear effect, Swan, Cummins and James (2001) studied two-dimensional surface water waves propagating on depth-varying currents. In the case of a following sheared current, it was observed that the water-particle velocities arising beneath a wave crest were substantially larger than those predicted by an irrotational wave-only solution.

Recently, Li, Troch and Rouck (2007) presented a Volume of Fluid (VOF) based flow solver using a finite-volume scheme and the sub-grid scale (SGS) turbulence model for the interactions between breaking waves and the current over a cut-cell grid. In the case of waves following the current, an external generator combining the inflow motions of the waves and the current is applied at the inflow boundary. In the case of waves in an opposing current, an internal generator is used to describe the opposing current by adding source functions in the mass and the momentum equations. The RANS-VOF method solves the Reynolds-Averaged Navier-Stokes (RANS) equations, on a fixed mesh and uses the VOF method to capture the free surface. Zhang *et al.* (2014a, 2014b) applied a RANS-VOF solver to study the solitary wave propagation in the presence of a steady current.

Most studies using RANS models, e.g. Li, Troch and Rouck (2007), Peng, Ma and Gu (2014), Zhang *et al.* (2014a, 2014b), have focused on waves interacting with a uniform current. Markus *et al.* (2013a, 2013b) used RANS-VOF to study the loading of waves and depth-varying currents on structures.

The objective of the paper is to examine the combined effects of wave nonlinearity and current shear on the water surface profiles. The numerical model is based on a Navier-Stokes solver and the VOF surface capturing scheme. Relaxation zones are employed to ensure the proper wave and current generation and wave absorption at the inlet and outlet. The numerical model is validated with the experimental measurements in the case of a uniform current and a linearly sheared current. The combined effects of wave nonlinearity and current shear are examined. Both following and opposing current are considered.

METHODOLOGY

Governing Equations

The fluid motion is assumed to be governed by the Navier-Stokes equations for an incompressible fluid. The mass continuity and momentum equations read

$$\nabla \cdot \mathbf{U} = 0 \quad (1)$$

$$\frac{\partial \rho \mathbf{U}}{\partial t} + \nabla \cdot (\rho \mathbf{U}\mathbf{U}) - \nabla \cdot (\mu_{eff} \nabla \mathbf{U}) = -\nabla p^* - \mathbf{g} \cdot \mathbf{X} \nabla \rho + \nabla \mathbf{U} \cdot \nabla \mu_{eff} \quad (2)$$

where $\mathbf{U}$ is the velocity vector, ρ is the density, p^* is the pseudo-dynamic pressure, $\mathbf{g}$ is the acceleration due to gravity, $\mathbf{X}$ is the position vector, $\mu_{eff} = \mu + \rho \upsilon_t$ is the effective dynamic viscosity, which takes into account of molecular dynamic viscosity μ and the turbulent eddy viscosity υ_t.

The two immiscible fluids of air and water are considered as one effective fluid and solved simultaneously throughout the domain, where the volume fraction α acts as an indicator function to mark the location of the interface of two different fluids. The indicator function is defined as: $\alpha = 1$ if the cell is full of water, $\alpha = 0$ if the cell is full of air, and $0 < \alpha < 1$ if the cell is a mixture of the two fluids. Using the indicator function, the local density ρ and the local viscosity μ of the fluid in each cell are given by

$$\rho = \alpha \rho_1 + (1-\alpha)\rho_2 \quad (3)$$

$$\mu = \alpha \mu_1 + (1-\alpha)\mu_2 \quad (4)$$

where the subscripts 1 and 2 denote water and air, respectively.

The scalar field of the indicator function is tracked by the advection equation (Weller, 2002)

$$\frac{\partial \alpha}{\partial t} + \nabla \cdot (\mathbf{U}\alpha) + \nabla \cdot [\mathbf{U}_c \alpha (1-\alpha)] = 0 \quad (5)$$

where an extra compression term is added to the classic VOF transport equation (Hirt and Nichols, 1985) to limit the smearing of the interface. This artificial convective term is active only in the thin interface region because of the multiplication term $\alpha(1-\alpha)$ and vanishes at both limits of the indicator function. More details about the VOF method can be found in Rusche (2002).

Numerical Methods

As the present study is focused on the current shear effect on regular non-breaking waves, the flow is assumed laminar and no turbulence models were used in the studies reported in this paper. Without resorting to the turbulence modeling, Eqs. 1~5 complete the mathematical description of the two-phase flow problem and are solved using a finite volume discretization and the PISO (Pressure Implicit with Splitting of Operators) algorithm. Details are thoroughly explained and applied for VOF in Jasak (1996).

In the present study, an extended version of the two-phase flow Navier Stokes solver (Jacobsen, Fuhrman and Fredsøe, 2012), the waves2Foam package, is used to investigate the wave-current interaction problem. This package has the added functionality of water wave generation with various wave theories and wave absorption using the relaxation zone technique. The implementation of a numerical wave-current interaction flume is relatively straightforward under this framework.

Model Setup

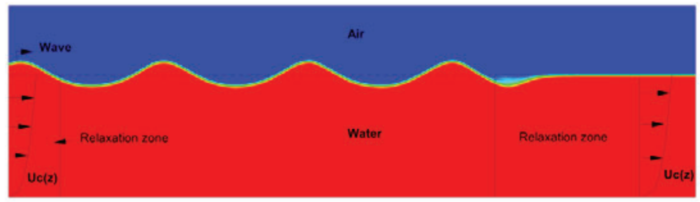

Fig. 1 Schematic of the 2D numerical wave-current flume

A numerical wave current flume was developed to investigate the changes that occur to the nonlinear regular waves when they propagate into a steady current field. Fig. 1 presents a sketch of the computational domain of the numerical flume. To minimize the contamination of wave reflection, a relaxation zone (Jacobsen, Fuhrman and Fredsøe, 2012) is introduced at both inlet and outlet to dissipate reflected wave energy in this region.

To avoid numerical instabilities that may occur due to the sudden wave generation, a cosine ramping function was applied to the wave component velocities and surface elevations specified at the inlet. By doing so, a series of waves are slowly built up and propagate into an existing steady current field. The wave-current interaction is hence captured within the computational domain as part of the CFD solution. The current effect on waves can be examined thereafter.

RESULTS AND DISCUSSIONS

In this section, the implementation of the numerical wave current flume is validated first with a uniform current, and then with a linearly sheared current. The numerical model results are compared with the experimental measurements in Swan (1990). The wave and current conditions used in Swan (1990) are tabulated in Table 1. The first two cases (1F and 1A) have a uniform current profile, while the other two cases (2F and 2A) have approximately a linearly sheared current profile. All cases deal with a relatively steep regular wave interacting with a steady current field. The wave steepness listed in Table 1 is calculated using the Doppler shifted nonlinear analytical solution according to Fenton (1985). For the case of sheared currents, an equivalent depth-averaged current velocity was used.

The numerical wave current flume has a length of 12 m and an air domain height of 0.25 m. The finite volume disretization of the domain is carried out using a Cartesian mesh. The base mesh size of the computational domain is 0.01 m in both horizontal and vertical directions. At the free surface area, the base mesh is refined once resulting into a smaller grid size. Overall, the computational domain has approximately 0.1 million cells. The model was run parallel using 4 cores (3.4 GHz) for 25 s. The simulation time varied from 3 hours to 10 hours depending on the case. The surface elevations and wave velocities presented in the following subsections were collected in the middle of the flume.

Table 1. Wave and current conditions

Case	Wave height H (m)	Water depth d (m)	Wave period T (s)	Wave steepness $0.5Hk$	Current profile
1F	0.0702	0.35	1.412	0.087	Uniform, following 0.108 m/s
1A	0.0714	0.45	0.877	0.218	Uniform, opposing -0.120m/s
2F	0.063	0.35	1.418	0.075	Linear shear, following [a]
2A	0.123	0.35	1.420	0.185	Linear shear, opposing [b]

a Refer to Fig. 2 (a).
b Refer to Fig. 2 (b).

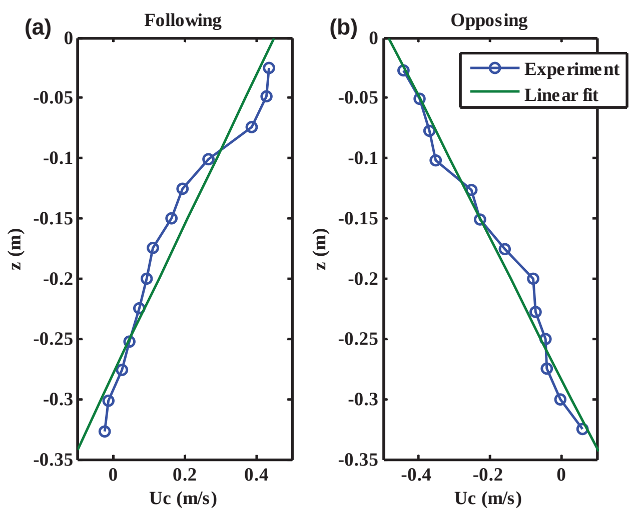

Fig. 2 Measured shear current profiles in Swan (1990). (a) case 2F: linearly sheared following current; (b) case 2A: linearly sheared opposing current.

Uniform Current

Fig. 3 presents the comparison of wave motions under a uniform, following current (case 1F) between experiment and the present numerical results, while Fig. 4 presents the comparison for the uniform, opposing current (case 1A). The oscillating wave component velocities were obtained by averaging out the mean velocities at each depth. The present model predictions of both the magnitude and phase of the surface elevation are in good agreement with experiment.

In Fig. 4(d), the extra red line indicates the numerical prediction by Son and Lynett (2014). It was noted in their paper that the error is likely due to the relatively large kd value for this case ($\approx$2.91). In contrast to their depth-integrated models in which long wave approximation is assumed, the present model is based on solving the Navier-Stokes equations without these constraints, therefore better agreement was achieved.

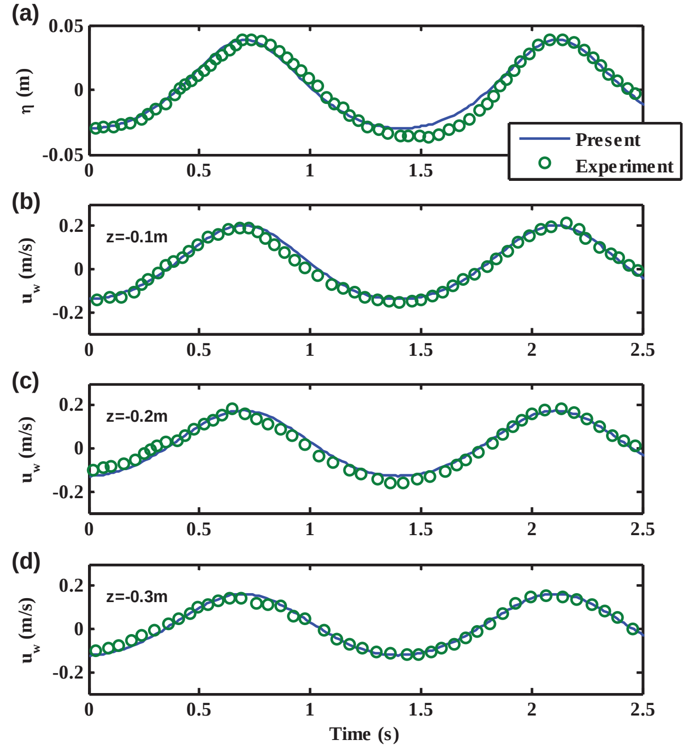

Fig. 3 Predicted (-) and observed (o) surface elevation (a) and horizontal wave velocities (b)-(d) under uniform, following current (case 1F).

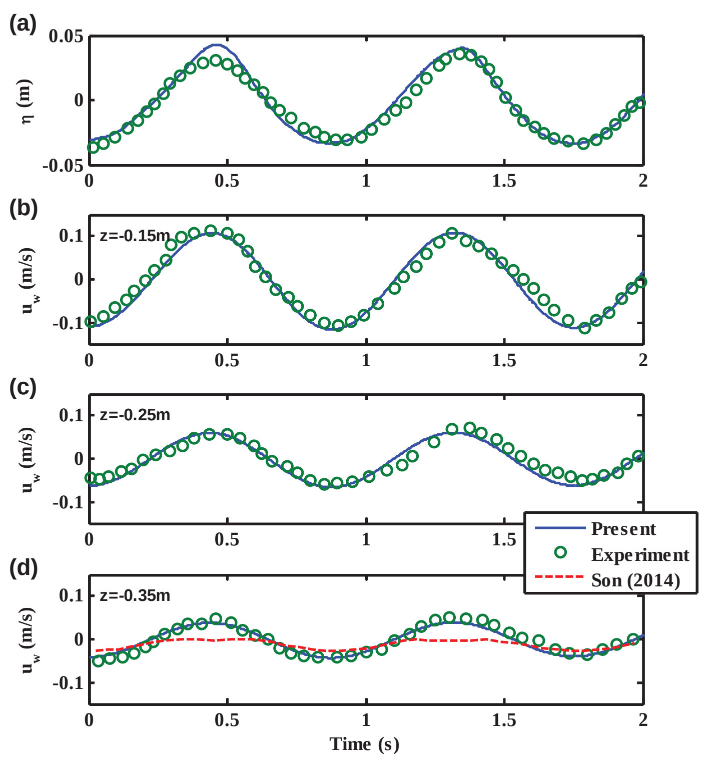

Fig. 4 Predicted (-) and observed (o) surface elevation (a) and horizontal wave velocities (b)-(d) under uniform, following current (case 1A).

Linearly Sheared Current

Fig. 5 presents the comparison of wave motions under a linearly sheared, opposing current (case 2A). Good agreement is achieved overall between the numerical results and the experimental measurements.

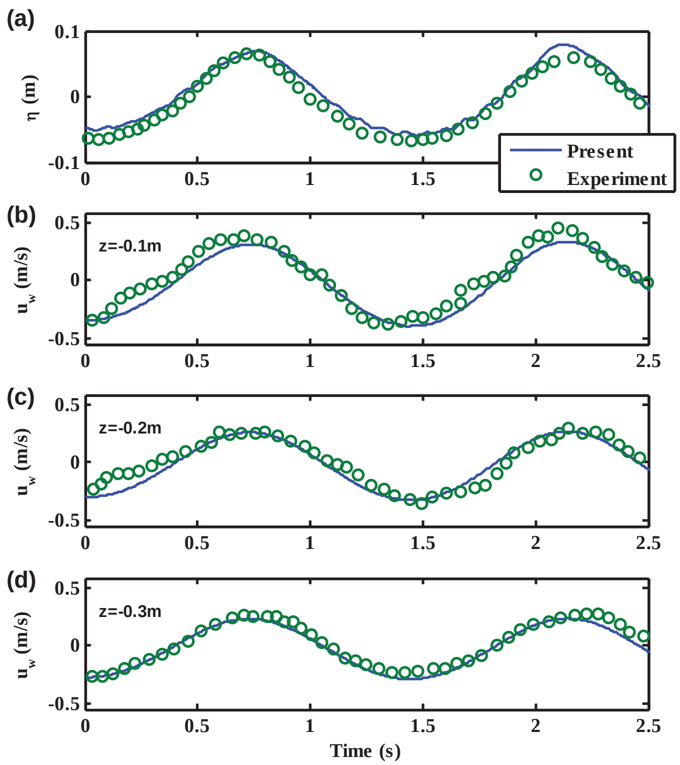

Fig. 5 Predicted (-) and observed (o) surface elevation (a) and horizontal wave velocities (b)-(d) under linearly sheared opposing current (case 2A).

Current Shear Effects on Wave Profiles

Cases 2F and 2A have almost the same wave period, but the wave height for case 2A is about twice that for case 2F. The two current profiles shown in Fig. 2 have approximately the same surface current velocity and current shear across the water depth. Combinations of the two waves and the two current profiles provide the opportunity to examine the combined effects of wave nonlinearity and current shear on the water surface profiles.

Fig. 6 presents the comparison of water surface elevations under different following current conditions for two wave heights, H=0.063 m and H=0.123 m, respectively. The present numerical model was run under the linearly sheared current and an equivalent uniform current, the magnitude of which is the average over water depth of the linearly sheared current profile. Also imposed on these plots are the analytical solutions by Fenton (1985) in absence of current.

It is most noticeable that due to the presence of the shear, the waves have relatively sharper crests and flatter troughs than those in uniform currents. This phenomenon is becoming more pronounced when the wave height is doubled, i.e. wave steepness doubled, as seen from Fig. 6(a) to 6(b). The maximum crest elevation for the large wave height case increases about 50% compared with the corresponding current-free case.

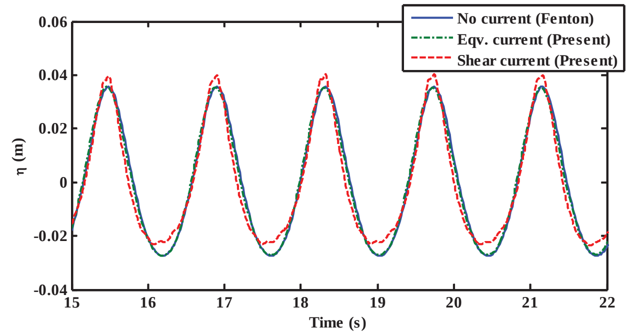

(a) H=0.063 m

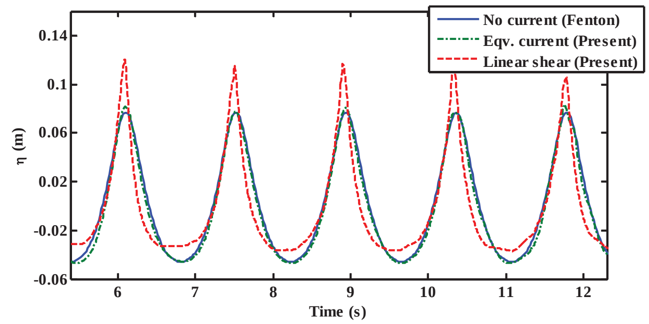

(b) H=0.123 m

Fig. 6 Current shear effect on water surface elevations (following current). Solid: analytical no current, wave-only solution (Fenton, 1985); dash-dot: prediction with equivalent uniform current; dashed: prediction with linearly sheared current.

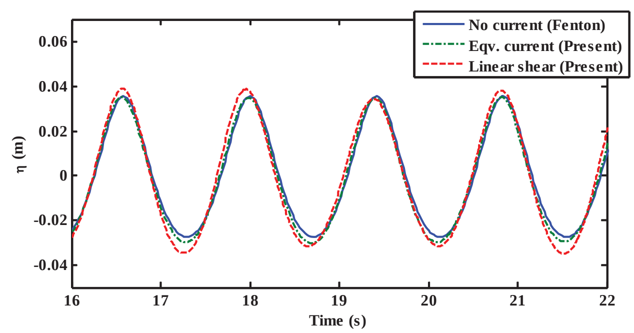

(a) H=0.063 m

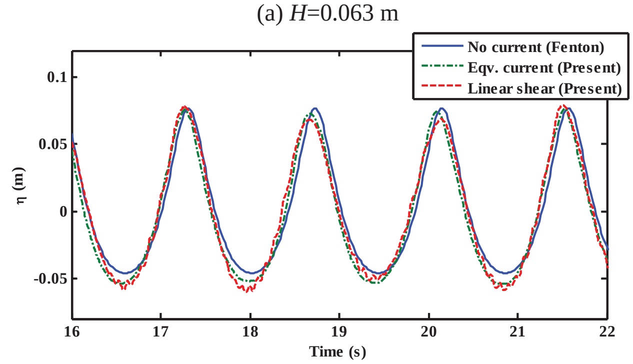

(b) H=0.123 m

Fig. 7 Current shear effect on water surface elevations (opposing current). Solid: analytical no current, wave-only solution (Fenton, 1985); dash-dot: prediction with equivalent uniform current; dashed: prediction with linearly sheared current.

Fig. 7 shows the comparison of water surface elevations under different opposing current conditions for two wave heights, H=0.063 m and H=0.123 m, respectively. The present numerical model was also run under the linearly sheared current and an equivalent uniform current. It is evident that the trough deepens in the presence of the current shear.

Comparing the wave surface elevation changes in Figs. 6 and 7, one can observe that there is a remarkable change in the crest elevation in presence of a linearly sheared following current, while the changes in the crest and trough is less visible when it comes to a linearly sheared opposing current. The elevated sharper crest and flatter trough in Fig. 6(b) greatly increases the asymmetry of the wave form. The asymmetry is due to nonlinear wave interactions, and therefore, is a measure of wave nonlinearity. The increased crest-trough asymmetry is most likely due to the significant wave-current interactions in presence of current shear. Energy transfer between the primary wave and the higher harmonics may also play a role in this process.

CONCLUSIONS

In this paper a numerical CFD model is presented to study the nonlinear wave interactions with sheared current profiles. The numerical model is validated in the case of a uniform current and a linearly sheared current. The effects of wave nonlinearity and current shear on the water surface profiles are examined. It was found that in the presence of the current shear, the wave crests are sharper and troughs flatter for the following current; while for the opposing current, the troughs tend to be deeper. The combinations of wave nonlinearity and current shear have stronger effect for following current than for opposing current. The effect is more pronounced when the wave steepness increases.

ACKNOWLEDGEMENTS

The authors would like to thank for the support by the start-up fund of University of Maine, the Physical Oceanography Program of National Science Foundation under Award Number 1436642, the Maine Sea Grant and National Oceanic and Atmospheric Administration through a grant (NA10OAR4170072).

REFERENCES

Brevik, I (1980). "Flume experiment on waves and currents II. Smooth bed," *Coastal Engng* 4, 89-110.

Dalrymple, RA (1974). "Water waves on a bilinear shear current," In *Proc. 14th Conf. on Coastal Engng*, Hamburg (ed. B. L. Edge). ASCE, Vol. 1, pp. 626-641.

Fenton, JD (1985). "A fifth-order Stokes theory for steady waves," *J. Waterway, Port, Coastal & Ocean Engng*, ASCE 111, 216-234.

Hirt, CW and Nichols, BD (1981). "Volume of fluid (VOF) method for dynamics of free boundaries," *J. Comput. Phys.* 39, 201-225.

Jacobsen, NG, Fuhrman, DR, and Fredsøe, J (2012). "A wave generation toolbox for the open-source CFD library: OpenFoam®," *Int. J. Numer. Meth. Fluids*, 70, 1073-1088. doi: 10.1002/fld.2726

Jasak, H (1996). Error analysis and estimation for the finite volume method with applications to fluid flows. Ph.D. thesis, Imperial College of Science, Technology and Medicine.

Jonsson, IG (1990). *Wave-current interactions. In The Sea*, pp. 65-120. J. Wiley and Sons.

Kemp, PH and Simons, RR (1982). "The interaction between waves and a turbulent current: waves propagating with the current," *J. Fluid Mech.* 116, 227-250.

Kemp, PH and Simons, RR (1983). "The interaction between waves and a turbulent current: waves propagating against the current," *J. Fluid Mech.* 130, 73-89.

Kishida, N and Sobey, RJ (1988). "Stokes theory for waves on a linear shear current," *J. Engng Mech.* 114, 1317-1334.

Li, T, Troch, P, and Rouck, JD (2007). "Interactions of breaking waves with a current over cut cells," *J. Comput. Phys.* 223, 865–897.

Markus, D, Hojjat, M, Wüchner, R, and Bletzinger, KU (2013a). "A CFD approach to modeling wave–current interaction," *J. Offshore Polar* 23, 29–32.

Markus, D, Wüchner, R, and Bletzinger, KU (2013b). "A numerical investigation of combined wave–current loads on tidal stream generators," *Ocean Eng.* 72, 416–428.

Peng, B, Ma N and Gu, X (2014). "RANS Simulation on Wave Blocking and Breaking of Water Surface Waves Propagating on Current," *Proceedings of 33rd International Conference on Ocean, Offshore and Arctic Engineering*, San Francisco, California, USA, OMAE2014-23618.

Peregrine, D. H. and Jonsson, I. G. (1983). *Interaction of Waves and Currents.* Misc. Rep. No. 83-6. C.E.R.C., U.S. Army, Corps of Engineers.

Rusche, H (2002). Computational fluid dynamics of dispersed two-phase flows at high phase fractions. PhD thesis, Imperial College.

Son, S, and Lynett, P J (2014). "Interaction of dispersive water waves with weakly sheared currents of arbitrary profile," *Coastal Engineering*, 90, 64-84.

Swan, C (1990). "An experimental study of waves on a strongly sheared current profile," In *Proc. 22nd Intl Conf. on Coastal Engng*, Delft (ed. B. L. Edge). ASCE, Vol. 1, pp. 489-502.

Swan, C, Cummins, IP, and James, RL (2001). "An experimental study of two-dimensional surface water waves propagating on depth-varying currents. Part 1. Regular waves," *Journal of Fluid Mechanics*, 428, 273-304.

Tsao, S (1959). "Behaviour of surface waves on a linearly varying flow," *Tr. Mosk. Fiz.-Tekh. Inst. Issled. Mekh. Prikl. Mat.* **3**, 66-84.

Thomas, GP (1981). "Wave-current interactions: an experimental and numerical study. Part 1. Linear waves," *J. Fluid Mech.* 110, 457-474.

Thomas, GP (1990). "Wave-current interactions: an experimental and numerical study. Part 2. Nonlinear waves," *J. Fluid Mech.* 216, 505-536.

Thomas, GP and Klopman, G (1997). "Wave-current interactions in the nearshore region," In Gravity Waves in Water of Finite Depth (ed. J. N. Hunt), *Computational Mechanics Publications*, pp. 215-319.

Umeyama, M (2005). "Reynolds stresses and velocity distributions in a wave-current coexisting environment," *J. Waterway, Port, Coastal, Ocean Eng.*, 131(5), 203–212.

Umeyama, M (2009). "Changes in turbulent flow structure under combined wave-current motions," *J. Waterw. Port Coast. Ocean Eng.* 135, 213-227.

Weller, HG (2002). Derivation, modelling and solution of the conditionally averaged two-phase flow equations. Technical Report TR/HGW/02, OpenCFD Ltd.

Zhang, JS, Zhang, Y, Jeng, DS, Liu, PLF, and Zhang, C (2014a). "Numerical simulation of wave–current interaction using a RANS solver," *Ocean Eng.*, 75, 157–164.

Zhang, J, Zheng, J, Jeng, DS, and Guo, Y (2014b). "Numerical Simulation of Solitary-Wave Propagation over a Steady Current," *J. Waterw. Port Coast. Ocean Eng.* 04014041-1-10.